(Figure 7), weak absorption can be observed (Figure 9). If this absorption is assigned to a $S_1 \rightarrow S_n$ transition in the merocyanine isomer(s), then its absence indicates that the S_1 lifetime in cyclohexane is so short that no significant S_1 population can be produced given the pumping conditions used. In general, this rationale suggests that a shortening of the S_1 lifetime in the merocyanine isomer(s) accounts for the weakening of the 400-460-nm absorption in nonpolar solvents.

Concluding Remarks

A reaction mechanism describing photochromism in SNP without a nitro group can be developed on the basis of the results presented here (Figure 8). This same mechanism also may have validity for other spiro compounds without a nitro group.

The initial ring opening appears unidirectional (i.e., irreversible) since the photolytic population of an excited electronic state in the merocyanine isomer(s) via double excitation experiments (Figure 6) does not result in any back-reaction to the SNP. Conversion from the merocyanine form to the original SNP seems to occur only thermally. The optical population of the S_1 state in the merocyanine isomer(s) by 574-nm excitation is confirmed through the 400-460-nm absorption observed by double excitation experiments (Figure 5). The effectiveness with which the merocyanine S_1 state is populated as well as its excited-state lifetime are strongly influenced by the solvent polarity (Figure 5), with polar solvents providing an environment in which the merocyanine S_1 state is more stable.

In a recent study, the merocyanine isomers produced from spirooxazines have been shown through PTR[3] data to equilibrate into different distributions (perhaps in some cases containing only one isomer) depending on the solvent.[18] These results suggest that the photochromism mechanism may involve several pathways which are influenced by interactions with the solvent. The observed changes in the 400-460-nm transient absorption reported here for SNP may reflect analogous solvent influences on the excited-state reaction mechanism. From such a perspective, the intermolecular interactions provided by the solvent environment may influence the excited-state relaxation properties and thereby change the photochemical reaction pathway and the merocyanine isomer(s) formed.

Registry No. SNP, 137668-57-6; merocyanine isomer, 137668-58-7.

Unusual 1:2 Ligand:Metal Complex Formation between an Anthraquinone Cryptand and Li^+

Zhihong Chen, Otto F. Schall, Mónica Alcalá, Yi Li, George W. Gokel,* and Luis Echegoyen*

Contribution from the Department of Chemistry, University of Miami, Coral Gables, Florida 33124. *Received July 22, 1991*

Abstract: A new cryptand containing an integral anthraquinone unit, **2**, has been synthesized. Electrochemical reduction of **2** in MeCN showed the two expected quasi-reversible waves at −1.03 and −1.40 V vs Ag/AgCl. Upon addition of 1 equiv of Li^+, a total of six reduction waves could clearly be seen at −0.44, −0.69, −0.97, −1.07, −1.31, and −1.48 V. The six waves correspond to the two electron reduction processes leading to the dianionic state of each of the three forms of the ligand: the free cryptand, the 1:1 complex, and 1:2 L:Li^+ complex. This is the first time that a 1:2 complex of this type has been detected by cyclic voltammetry. The existence of this 1:2 complex ($\mathbf{2}^{\bullet-}$:2Li^+) was confirmed by ESR spectroscopy and by a binding study using ^{7}Li NMR. The binding constant for this 1:2 complex was found to be 1.7×10^2, but this value was increased to 1.0×10^8 upon one-electron reduction and to 1.3×10^{13} upon two-electron reduction. Even in the presence of only 1 equiv of Li^+/equiv of $\mathbf{2}^{\bullet-}$, the ESR spectrum shows a hyperfine splitting from two equivalent Li^+ cations of 0.20 G. A possible structure for this 1:2 complex is proposed, in which the two cations interact with the same carbonyl group on the anthraquinone, while they are simultaneously solvated by the enveloping crown ether. 1:2 complex formation with Na^+ and K^+ has also been detected by using voltammetry and ESR. Since hyperfine coupling from only one cation is resolved, an unsymmetric complex is proposed. In this structure, the cation exhibiting the hyperfine splitting is inside the cryptand cavity. The other is assumed to be interacting with the external carbonyl and to be in relatively fast exchange with the solvent. While the $\mathbf{2}^{\bullet-}$:Na^+ complex can be dissociated by addition of cryptand [2.2.1], $\mathbf{2}^{\bullet-}$:K^+ complex cannot be fully dissociated by addition of cryptand [2.2.2]. This implies that reduced **2** is at least as good a K^+ binder as cryptand [2.2.2].

Introduction

For a number of years we have been interested in podands, macrocycles, and macrobicycles capable of exhibiting coupling between a redox reaction and a cation binding process.[1-5] The molecules are designed to show cation binding properties even in the absence of the redox process. Thus, they all have an acyclic (podand),[6] cyclic (crown),[7] or bicyclic (cryptand)[8] poly(oxyethylene) structure. An electroactive group is present in close to and in the proper geometrical orientation with respect to the cation binding center. Electrochemical (or chemical) reduction of the ligands then leads to excess negative charge which in turn enhances the binding of the cation. Binding enhancement values between

(1) Kaifer, A.; Echegoyen, L.; Gustowski, D. A.; Goli, D. M.; Gokel, G. W. *J. Am. Chem. Soc.* **1983**, *105*, 7168.
(2) Gustowski, D. A.; Echegoyen, L.; Goli, D. M.; Kaifer, A.; Schultz, R. A.; Gokel, G. W. *J. Am. Chem. Soc.* **1984**, *106*, 1633.
(3) Morgan, C. R.; Gustowski, D. A.; Cleary, T. P.; Echegoyen, L.; Gokel, G. W. *J. Org. Chem.* **1984**, *49*, 5008.
(4) Kaifer, A.; Gustowski, D. A.; Echegoyen, L.; Gatto, V. J.; Schultz, R. A.; Cleary, T. P.; Morgan, C. R.; Goli, D. M.; Rios, A. M.; Gokel, G. W. *J. Am. Chem. Soc.* **1985**, *107*, 1958.
(5) Echegoyen, L.; Gustowski, D. A.; Gatto, V. J.; Gokel, G. W. *J. Chem. Soc., Chem. Commun.* **1986**, 220.
(6) Gustowski, D. A.; Delgado, M.; Gatto, V. J.; Echegoyen, L.; Gokel, G. W. *Tetrahedron Lett.* **1986**, *27*, 3487.
(7) Delgado, M.; Echegoyen, L.; Gatto, V. J.; Gustowski, D. A.; Gokel, G. W. *J. Am. Chem. Soc.* **1986**, *108*, 4135.
(8) Gustowski, D. A.; Gatto, V. J.; Kaifer, A.; Echegoyen, L.; Godt, R. E.; Gokel, G. W. *J. Chem. Soc., Chem. Commun.* **1984**, 923.

0002-7863/92/1514-444$03.00/0

10^2 and 10^6 have been reported.[1-8] The binding of the cation and the redox process are thus coupled. Since the redox process is reversible, a switch is present which allows control between low and high cation binding states.[9]

The anthraquinone group has proven to be the most versatile and useful redox-active group in these studies.[5-7] Others have also prepared crown ether derivatives containing anthraquinone groups for cation binding–redox coupling.[10] Still others have shown that lipophilic anthraquinones (a dipalmitoylphosphatidylcholine derivative of anthraquinone) can act as electron, and H^+ shuttles across lipid bilayers.[11]

Our work has amply shown that these ideas can be used to enhance cation binding reversibly[1-9] as well as to enhance cation transport across bulk liquid membranes.[12] Cation-transport enhancement results from the same principle: A redox gradient across the membrane favors the ligand's high binding state at one of its interfaces (the reducing side), while the low binding state is favored in the oxidizing side. The result is cation "pumping" across the membrane, in favor of the redox gradient.

The major problem that we have encountered in this work is the lack of cation binding selectivity of these ligands once they are reduced.[13] Most polyether ligands exhibit binding preference for K^+ over Na^+ and for Na^+ over Li^+.[14] Upon electrochemical reduction, the enhancement factors exhibit the reverse order, as expected based on the charge densities of these cations. The net result is a leveling effect of the cation binding strengths and a consequent loss of binding selectivity. The only exception to this behavior that we are aware of was exhibited by an azo cryptand,[8] the only redox-active macrobicycle that we have studied, **1**. This compound is the only example exhibiting K^+ (over Na^+ or Li^+) selectivity upon electrochemical reduction.

In an effort to construct systems which are redox switchable and somewhat more selective, we report here the synthesis, cation binding, electrochemistry, and ESR spectra of a new, anthraquinone-containing cryptand, **2**. To our knowledge, this is the first time that an anthraquinone group has been incorporated directly into a cryptand structure.

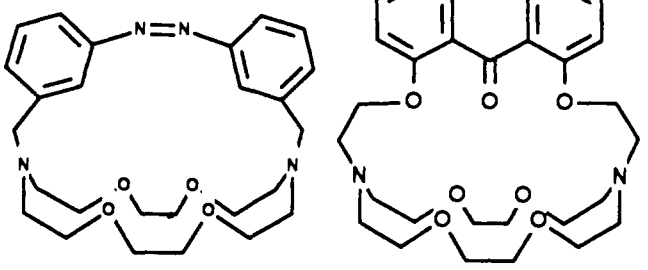

1

2

Experimental Section

General Procedures. ^1H NMR spectra were recorded at 399.95 MHz in $CDCl_3$. Chemical shifts (δ) (ppm) downfield from internal Me_4Si (TMS) are reported in the following order: chemical shift, peak multiplicity (broad; s = singlet; d = doublet; t = triplet; m = multiplet), integration, and assignment. Infrared (IR) spectra were recorded as KBr pellets (cm^{-1}), calibrated against the 1601-cm^{-1} band of polystyrene. Melting points were determined on a capillary melting point apparatus and are uncorrected. Combustion analyses were performed at Atlantic Microlab, Inc., Atlanta, GA. Thin-layer chromatographic analyses were performed on aluminum oxide 60 F-254 neutral (type E) or on silica gel 60 F-254. Preparative chromatographic columns were packed with aluminum oxide (activated, neutral, 150 mesh), standard grade, or with Kieselgel 60 (70–230 mesh). All reactions were conducted under dry N_2. All reagents were of the best grade available commercially and were used without further purification, unless otherwise indicated.

Reagents and Solvents. Many of the experimental details have been reported previously.[15] All solutions were prepared under a dry N_2 atmosphere or under vacuum (10^{-3} mm). Tetrabutylammonium perchlorate (TBAP; Fluka) was recrystallized first from EtOAc and then from deionized water (Barnsted Nanopure 18 MΩ) and dried in vacuo for 24 h at 110 °C. All alkali-metal cations were added to the solutions as their corresponding perchlorates or as the tetraphenylborate. These salts (Aldrich) were recrystallized from deionized water and dried in a vacuum oven at 100 °C for 24 h. Acetonitrile (Alfa) was first distilled from CaH_2 and then from P_2O_5 prior to use. Deuterated acetonitrile (MeCN-d_3) was used directly as received from Aldrich. Tetrahydrofuran (THF; Aldrich) was purified over CaH_2 and then distilled and kept over Na:2K under vacuum until needed. It was flask to flask distilled from Na:2K directly through a vacuum line and into the reaction cell for use.

Preparation of 1,8-Bis(2-bromoethoxy)anthraquinone. To a solution of 1,8-dihydroxyanthraquinone (5 g, 20.8 mmol) in anhydrous DMF (80 mL) was added Cs_2CO_3 (30 g, 92 mmol) with stirring over 10 min. A color change from orange to deep purple was observed. Dibromoethane (10 mL, 116 mmol) was added, and the mixture heated to 80 °C. After 3 h, the reaction mixture was cooled and filtered through a pad of Celite and the solvent removed in vacuo to afford, after column chromatography (SiO_2, 0–4% MeOH–CH_2Cl_2) and crystallization from EtOAc, the dibromide (3.2 g, 18%) as long orange needles: mp 153–154 °C; ^1H NMR 3.76 (t, 4 H, CH_2Br), 4.44 (t, 4 H, $ArOCH_2$), 7.31 (d, 2 H, Ar H2 and H7), 7.62 (t, 2 H, Ar H3 and H6), 7.87 (d, 2 H, Ar H4 and H5). Anal. Calcd for $C_{18}H_{14}Br_2O_2$: C, 47.61; H, 3.11. Found: C, 47.51; H, 3.13.

Preparation of Anthraquinone [2.2] Cryptand (2). A solution of 4,13-diaza-18-crown-6 (1.0 g, 3.8 mmol) in *n*-PrCN (50 mL) was added to a solution of the dibromide (see above; 1.74 g, 3.8 mmol) in 350 mL of the same solvent, containing Na_2CO_3 (9.6 g, 91 mmol) and NaI (0.7 g, 4.7 mmol). The suspension was stirred and heated at 100 °C for 24 h, cooled, and filtered and the solvent removed in vacuo, to afford a greenish oil. Column chromatography (Al_2O_3, 0–1% MeOH–$CHCl_3$) followed by recrystallization from absolute EtOH (20 mL) afforded **2** (1.1 g, 52%) as green crystals: mp 127–129 °C, turned brown; ^1H NMR 3.05 (t, 8 H, CH_2NCH_2 in crown), 3.31 (t, 4 H, N[crown]CH_2), 3.61 (broad s, 8 H, OCH_2CH_2O), 3.72 (m, 8 H, OCH_2CH_2N), 4.18 (t, 4 H, $ArOCH_2$), 7.24 (d, 2 H, Ar H2 and H7), 7.58 (t, 2 H, Ar H3 and H6), 7.89 (d, 2 H, Ar H4 and H5); IR 3440 (br), 2980, 2900, 2840, 1680, 1595, 1480, 1460, 1450, 1420, 1365, 1330, 1270, 1250, 1180, 1140, 1120, 1105 cm^{-1}. Anal. Calcd for $C_{30}H_{38}N_2O_8$: C, 64.97; H, 6.91; N, 5.05. Found: C, 64.72; H, 6.93; N, 4.99.

Electron Spin Resonance. ESR spectra were recorded by using the X-band of an IBM ER200 SRC spectrometer equipped with a TE_{104} rectangular cavity. The instrument was controlled with an IBM 9000 computer. Alkali-metal reductions were conducted under vacuum (10^{-3} mm) in dry THF for solutions containing ~1 mM **2**. After reduction with either Na^0 or K^0, the spectra were recorded for the corresponding complexes, $2^{\bullet-}$:M^+. Reduction with Li^0 was too slow to be useful. Therefore, $2^{\bullet-}$:Li^+ was not prepared in the same manner; vide infra. The spectrum of the reduced ligand in the absence of an interacting cation was obtained by the addition of an excess amount of cryptand [2.2.1] to the solution resulting from the Na^0 reduction. In this manner it was possible to sequester the cation away from the anion radical of **2**. A similar treatment of a K^0-reduced solution with cryptand [2.2.2] did not yield the spectrum of the unassociated anion radical. Additions of cryptands and alkali-metal perchlorate salts to these anion-radical solutions were conducted using break seals, as previously described.[15]

In order to study the interactions of $2^{\bullet-}$ with Li^+ it was necessary to generate the anion radical via electrolytic reduction. Reductions were performed under Ar, using dry MeCN solutions with 0.1 M TBAP, using a BAS-100 electrochemical analyzer system. A Pt mesh electrode (3 × 3 cm) was used as the working electrode and a Pt plate as a counter electrode, with a Ag wire as a pseudoreference. The potential was controlled at −1.0 V, and the electrolysis was stopped after the current had decreased to 20% of its initial value. The solution was then transferred

(9) Gustowski, D. A.; Delgado, M.; Gatto, V. J.; Echegoyen, L.; Gokel, G. W. *J. Am. Chem. Soc.* **1986**, *108*, 7553.

(10) Ozeki, E.; Kimura, S.; Imanishi, Y. *J. Chem. Soc., Chem. Commun.* **1988**, 1353.

(11) Liu, M. D.; Patterson, D. H.; Jones, C. R.; Leidner, C. R. *J. Phys. Chem.* **1991**, *95*, 1858 and references therein.

(12) (a) Echeverria, L.; Delgado, M.; Gatto, V. J.; Gokel, G. W.; Echegoyen, L. *J. Am. Chem. Soc.* **1986**, *108*, 6825. (b) Echegoyen, L. E.; Yoo, H. K.; Gatto, V. J.; Gokel, G. W.; Echegoyen, L. *J. Am. Chem. Soc.* **1989**, *111*, 2440. (c) Chen, Z.; Gokel, G. W.; Echegoyen, L. *J. Org. Chem.* **1991**, *56*, 3369.

(13) Kaifer, A.; Echegoyen, L. Redox Control of Cation Binding in Macrocyclic Systems. In *Cation Binding by Macrocycles: Complexation of Cationic Species by Crown Ethers*; Inoue, Y., Gokel, G. W., Eds.; Marcel Dekker: New York, 1990; Chapter 8, p 363.

(14) Echegoyen, L.; Gokel, G. W.; Echegoyen, L. E.; Chen, Z.; Yoo, H. *J. Inclusion Phenom.* **1989**, *7*, 257.

(15) Delgado, M.; Gustowski, D. A.; Yoo, H. K.; Gokel, G. W.; Echegoyen, L. *J. Am. Chem. Soc.* **1988**, *110*, 119.

Table I. Summary of Coupling Constants (G), for the Spectra of $2^{\bullet-}$ in the Absence and Presence of Different Cations (TSW Refers to the Total Spectral Width, and LW Is the Individual Line Width)

	a_1(2 H)	a_2(2 H)	a_3(2 H)	a_{M^+}	TSW	LW
none	0.65	0.75	1.54		5.88	0.21
Li^+	0.46	1.88		0.20[a]	5.88	0.16
$2Li^+$	0.46	1.88		0.20[a]	5.88	0.16
Na^+	0.35	1.12	1.20	0.35	6.39	0.16
$2Na^+$	0.70	0.86	1.44	0.70	8.10	0.25
K^+	0.27	1.14	1.14	0.11	5.43	0.14
$2K^+$	0.75	0.83	1.61		6.38	0.30

[a] Value corresponds to two equivalent Li^+ cations.

to a 3-mm ESR cell, all under Ar, and the ESR spectrum recorded.

Cyclic Voltammetry. The electrochemical experiments were performed at 25 °C under a dry N_2 atmosphere with MeCN solutions containing 0.1 M TBAP. The electroactive species was present in millimolar concentrations (1–3). A polished glassy carbon electrode was used as the working electrode and a Pt wire as the counter electrode, and Ag/AgCl served as the reference electrode. Measurements were also done with the BAS-100 system and recorded on a Houston DMP-40 plotter. Typical sweep rates were on the order of 100 mV/s. Alkali-metal perchlorate salts were added directly into the electrochemical cell by incremental amounts, while the voltammogram was recorded after each addition.

Binding Constant Determinations. Potentiometric Determinations Using a Competition Method with Ag^+. Potentiometric determinations were conducted following the procedure previously described in detail.[16] The reference electrode used was a Ag wire immersed in a Ag^+ solution of known concentration in MeCN. The two half-cells were separated by a salt bridge containing 0.05 M TBAP which made contact with the solutions via two Vycor tips.

The stability constants with Ag^+ were determined by simple potentiometric titrations of a ligand solution with a $AgNO_3$ solution. The ionic strength was kept constant at $I = 0.05$ M by addition of TBAP. The total ligand concentrations used were in the range of 5×10^{-4}–5×10^{-3} M, and Ag^+ concentrations were in the range of 10^{-4}–10^{-3} M. The concentration of free Ag^+ was measured with a Ag^0 wire electrode, potentials being measured with a digital ionalyzer (Orion Research Model 701A). The same experimental procedure was used to titrate a solution containing the ligand and another cation M^+. The stability constants for the other cations were obtained from the measurable concentration of the competing free Ag^+ and the known equilibrium constants for the Ag^+ complex. During a typical titration, the total metal ion concentration was 5×10^{-3} M and the total ligand concentration was 1×10^{-3} M, while the total Ag^+ concentration was varied between 5×10^{-5} and 8×10^{-4} M.

The method was calibrated by titrating cryptand [2.2.2] with Ag^+, Na^+, and K^+. All experiments were carried out under a dry N_2 atmosphere at 25 °C.

Direct ^{23}Na and ^{7}Li NMR Methods. ^{23}Na and ^{7}Li NMR measurements were carried out using a Varian VXR 400 spectrometer operating at 105.8 (^{23}Na) or 155.45 MHz (^{7}Li). Chemical shifts were referenced to 3 M aqueous NaCl or 4 M aqueous $LiClO_4$. Titrations were conducted in MeCN-d_3 with the ligand concentration constant. The value of the ligand concentration was 10 mM in the case of the titration with Na^+, and it was 5 mM for the Li^+ case. The cation concentration varied between 0 and 40 mM. A total of at least 13 spectra were recorded as a function of the added metal cation concentration in the course of a typical titration. All measurements were conducted at a constant probe temperature of 21 °C. Chemical shift (δ) vs ($2/M^+$) plots were fitted by a nonlinear regression analysis (program MINSQ). The model introduced in the program allowed for 1:1 as well as for 1:2 complex formation possibilities. These correspond to K_1 and K_2 in Scheme I.

Results and Discussion

ESR Experiments. The ESR spectrum of $2^{\bullet-}$ is presented in Figure 1, along with its computer simulation. The anion radical was generated via electrolytic reduction of the parent compound in MeCN, as described in the Experimental Section. An almost identical spectrum is obtained if **2** is reduced with Na^0 in THF and an excess of cryptand [2.2.1] is added to sequester the cation. It can therefore be concluded that this spectrum corresponds to the unassociated anion radical in solution. The coupling constants used for the simulation are summarized in Table I.

(16) Gustowski, D. A.; Gatto, V. J.; Mallen, J.; Echegoyen, L.; Gokel, G. W. *J. Org. Chem.* **1987**, *52*, 5172.

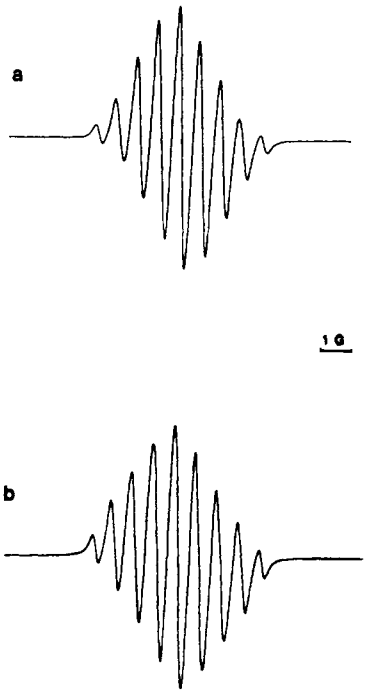

Figure 1. (a) ESR spectrum of $2^{\bullet-}$ in CH_3CN–TBAP, generated via electrolytic reduction on a Pt electrode. (b) Computer-simulated spectrum. All the coupling constant values used for the simulation can be found in Table I.

As expected, three sets of two equivalent hydrogen coupling constants are observed, with values of $a_{2H} = 0.65$, $a_{2H} = 0.75$, and $a_{2H} = 1.54$ G. These values are in perfect agreement with previously reported data for a somewhat analogous system, **3**.[15] The anion radical of **3** exhibited $a_{2H} = 1.54$ G, and the other two sets of two hydrogens were accidentally degenerate with $a_{4H} = 0.69$ G. The total spectral widths are essentially identical for $2^{\bullet-}$ and $3^{\bullet-}$, with values of 5.88 and 5.84 G, respectively. All of these parameters are summarized in Table I.

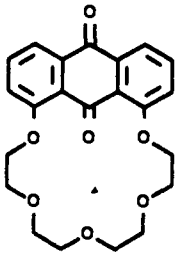

3

Addition of 1 equiv of Li^+ to a solution of $2^{\bullet-}$ resulted in the spectrum shown in Figure 2. Notice the pronounced spectral change relative to the spectrum in Figure 1, where the nine relatively broad lines have been substituted by a pattern clearly exhibiting a large triplet structure with multiple smaller hyperfine splittings which are very sharp. An almost perfect simulation of this new spectrum in the presence of Li^+ was accomplished using $a_{2H} = 1.88$, $a_{2H} = 0.46$, and, surprisingly, $a_{2Li} = 0.20$ G. All values are reported in Table I. The surprising observation is not the disappearance of one of the hydrogen sets nor the observation of a Li^+ hyperfine, since these have been also observed for $3^{\bullet-}$:Li^+.[15] The unexpected observation is the presence of two equivalent Li^+ splittings, particularly since only 1 equiv of the alkali-metal cation salt was added.

The only other case involving a reduced anthraquinone where a hyperfine splitting was observed from two equivalent alkali-metal cations was $4^{\bullet-}$:$2Na^+$.[15] In this case the interpretation given was that "each sidearm could coil over opposite sides of the anthraquinone residue so that each Na^+ is in a nearly tetrahedral environment and both cations share the carbonyl oxygen."[15] Such

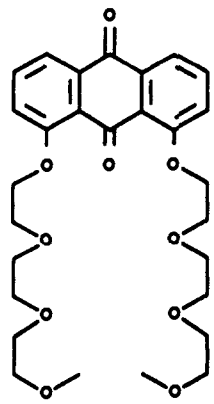

4

a description defines a three-dimensional structure for the triple-ion complex which is very similar to the actual structure for $\mathbf{2}^{\bullet-}$, the anthraquinone cryptand. The structural similarities between the two were judged on the basis of CPK models. Thus, it is reasonable to expect that two Li^+ cations would interact with $\mathbf{2}^{\bullet-}$ via interactions with the same carbonyl oxygen on the anthraquinone, while positioning themselves in the "side pockets" offered by the cryptand structure. This possibility must be much more favored than cryptation of the cation for the case of Li^+, as judged by the observation of the 1:2 complex even after addition of 1 equiv of the salt. This 1:2 complex formation has been confirmed by cyclic voltammetric experiments; vide infra.

In order to see if further addition of $LiClO_4$ resulted in more spectral changes, an additional 1 equiv of the salt was added to the solution exhibiting the spectrum shown in Figure 2. No spectral changes were noticeable, except for a slight broadening of the signals.

Addition of 1 equiv of Na^+ to a MeCN solution of $\mathbf{2}^{\bullet-}$ also results in drastic changes of the ESR spectrum; see Figure 3. The simulation clearly demonstrates that a sodium splitting is present, with a value of $a_{Na^+} = 0.35$ G. But notice that splitting from only one cation is observed. It is again instructive to compare the present results with those previously obtained with $\mathbf{4}^{\bullet-}$:Na^+.[15] For $\mathbf{4}^{\bullet-}$:Na^+ the following coupling constants were determined: $a_{2H} = 1.25$, $a_{2H} = 0.95$, $a_{2H} = 0.17$, $a_{Na^+} = 0.19$ G. The situation observed with $\mathbf{2}^{\bullet-}$:Na^+ is very similar, with three sets of two hydrogens each: $a_{2H} = 1.20$, $a_{2H} = 1.12$, and $a_{2H} = 0.35$ G and the sodium coupling of 0.35 G; see Table I. Further addition of an extra 1 equiv of Na^+ leads to spectral differences, but these are obscured by a simultaneous broadening of the lines; see Figure 3. The best simulation, which is also presented in Figure 3, was obtained using the coupling constants given in Table I. Notice that the spectrum is basically composed of 12 broad lines and that with so many splittings it is difficult to arrive at a unique set of coupling constants. Although the specific coupling constants are not entirely certain, we feel confident that a Na^+ hyperfine is present and that it corresponds to a single nucleus. Thus, the situation with Li^+ is specific to this cation and results from its smaller size. This enables it to fit well into these "side pockets", something impossible for the larger Na^+. It is thus probable that the Na^+ complex is of the cryptate variety, with the cation encapsulated by the reduced ligand and located directly underneath the quinone carbonyl. It should be noted that addition of a slight excess of cryptand [2.2.1] is able to compete effectively for all of the Na^+ present, and the original, unassociated anion radical spectrum is thus restored.

We believe that the changes observed upon addition of the extra 1 equiv of Na^+ are due to association with the quinone carbonyl which is outside of the cryptand cavity. Therefore, the observed Na^+ splitting corresponds to the cryptated cation, while the spectral changes associated with the second Na^+ equivalent, notably the line broadening, arise as a consequence of fast complexation–decomplexation with the outside carbonyl. This fast process broadens all of the spectral lines while it simultaneously changes the spin distribution of the complex, but without exhibiting an additional Na^+ splitting.

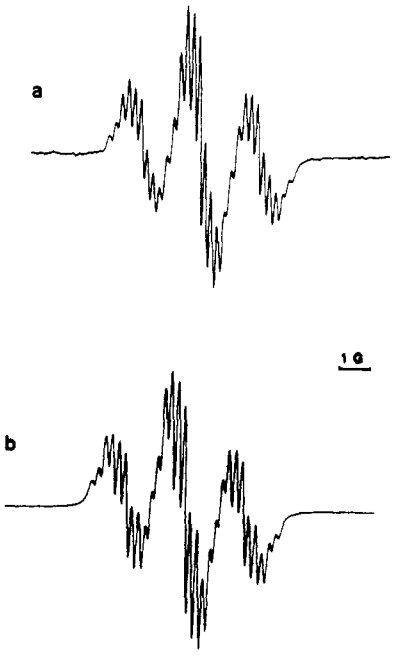

Figure 2. (a) ESR spectrum of $\mathbf{2}^{\bullet-}$ in the presence of 1 equiv of added Li^+. (b) Computer-simulated spectrum. Note: an identical spectrum is obtained if 2 equiv of Li^+ is added to a solution of $\mathbf{2}^{\bullet-}$. All the coupling constant values used for the simulation can be found in Table I.

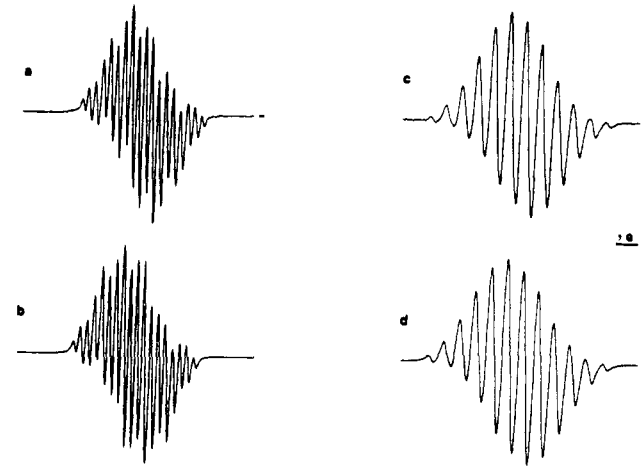

Figure 3. (a) ESR spectrum of $\mathbf{2}^{\bullet-}$ in the presence of 1 equiv of added Na^+. (b) Computer-simulated spectrum for (a). (c) ESR spectrum of $\mathbf{2}^{\bullet-}$ in the presence of 2 equiv of added Na^+. (d) Computer-simulated spectrum for (c). All the coupling constant values used for the simulations can be found in Table I.

Addition of 1 equiv of K^+ also results in pronounced spectral differences; see Figure 4. A pentet structure is evident, with $a_{4H} = 1.14$ G. The best simulation was obtained with an additional and small $a_{2H} = 0.27$ G and $a_{K^+} = 0.11$ G. Since the cryptand cavity is most appropriate for this cation, the nature of the complex is assumed to be inclusive. The smaller value of the metal hyperfine compared to the others is simply a reflection of the smaller value of its gyromagnetic ratio. Addition of an extra 1 equiv of $KClO_4$ leads to changes similar to those observed when 2 equiv of Na^+ is added, including the drastic increase in the line width; see Figure 4. No K^+ splitting can be seen, but this is probably due to the lack of resolution, since the observed line width is 0.30 G. The hydrogen coupling constants match those of the $2Na^+$ case quite well. This is a good indication that the electrostatic effect on **2** is similar in these two cases, the main difference being the much smaller value of the metal hyperfine in the case of K^+. We feel that the situation with the 2 equiv of K^+ added is similar to that of Na^+, where one K^+ is cryptated while the other one interacts with the outside carbonyl.

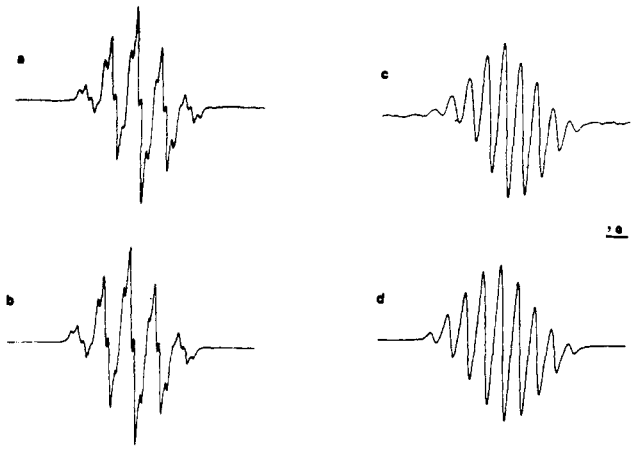

Figure 4. (a) ESR spectrum of $2^{\bullet-}$ in the presence of 1 equiv of added K^+. (b) Computer-simulated spectrum for (a). (c) ESR spectrum of $2^{\bullet-}$ in the presence of 2 equiv of added K^+. (d) Computer-simulated spectrum for (c). All the coupling constants used for the simulations can be found in Table I.

Scheme I

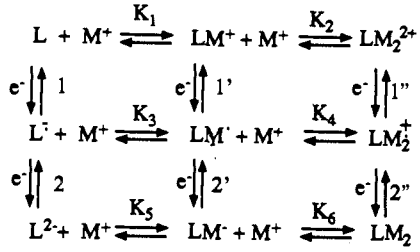

An interesting observation was that addition of a slight excess of cryptand [2.2.2] to the solution containing the K^+ complex did not result in an effective removal of the cation from the reduced complex, as observed for the Na^+ case using [2.2.1]. This is not totally unexpected and simply reflects the fact that the reduced ligand is able to compete effectively for K^+, even with cryptand [2.2.2].

One other thing must be pointed out with respect to the ESR spectra. As has been previously observed with $4^{\bullet-}$,[15] $2^{\bullet-}$ exhibits the largest total spectral width (TSW) increase when it is in the presence of 2 equiv of Na^+. The value is 8.10 G, which compares with 5.88 G for the free anion radical and with 8.98 G for $4^{\bullet-}$:2Na^+. With 1 equiv of Na^+, the value is 6.39 G. These TSW differences are mainly the result of the spin densities which are localized on the metal cations.

Cyclic Voltammetry. Based on the ESR results, it was hoped that the 1:2 ligand:Li^+ complex would be detectable by cyclic voltammetry. Previous studies with podand and crown anthraquinones had only resulted in a maximum observation of four reversible redox waves, two corresponding to the first and second electron reductions of the free ligand and the other two to the corresponding ones for the 1:1 complex. Referring to Scheme I, these redox processes are 1 and 2 for the free ligand and 1′ and 2′ for the 1:1 complex. If, as depicted in the scheme, the ligand can bind a second cation via a K_2 process, additional 1″ and 2″ redox processes should be observable for the 1:2 complex, for a total of six. Since K_2 should be very small, our expectation was that redox process 1″ should not be observed. This would lead to the observation of only five waves. The results clearly exceeded this expectation.

The cyclic voltammograms for **2** in MeCN are presented in Figure 5, as a function of added $LiClO_4$. In the absence of any added salt, the voltammogram exhibited the usual quasi-reversible waves corresponding to the two electron-transfer processes leading to the formation of the dianionic anthraquinone, processes 1 and 2 in scheme I. The second process, as has been found with other anthraquinone systems, is somewhat chemically and electrochemically irreversible.[5,6,9] Addition of 0.5 equiv of Li^+ leads to

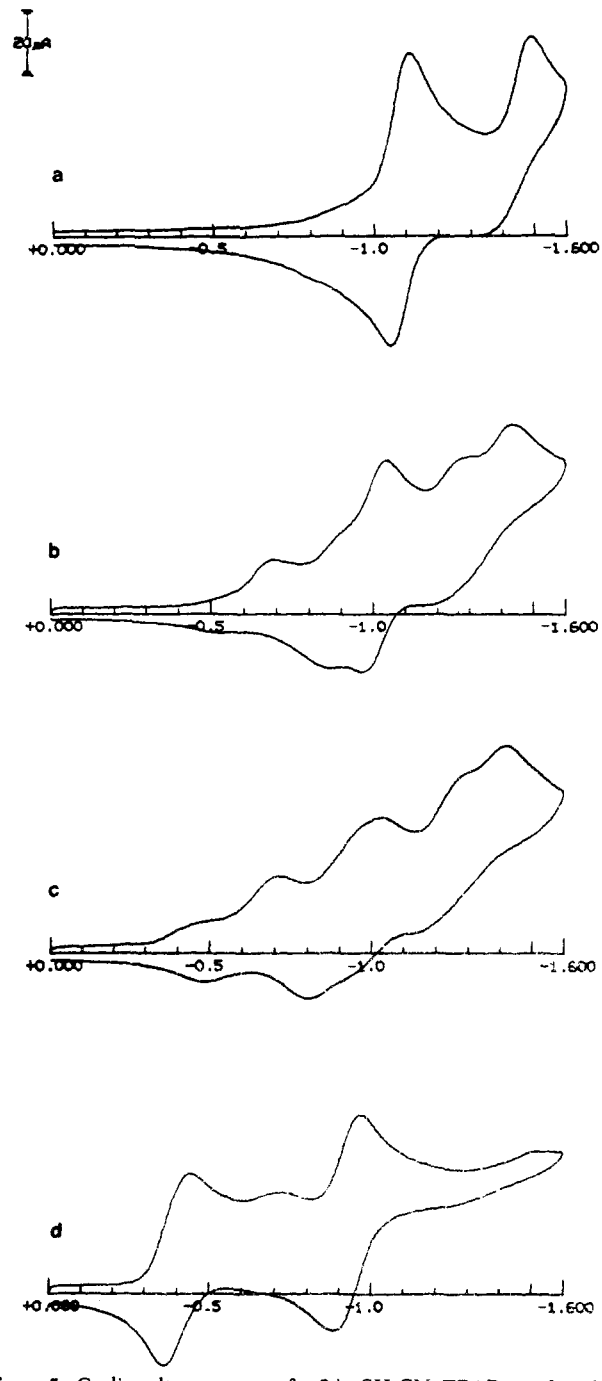

Figure 5. Cyclic voltammograms for **2** in CH_3CN–TBAP as a function of added $LiClO_4$: (a) no added Li^+, (b) 0.5 equiv of Li^+ added/equiv of **2**, (c) 1.0 equiv of Li^+ added, and (d) 2.0 equiv of Li^+ added. Potentials are referenced to a Ag/AgCl electrode.

the observation of an additional two (possibly three) reduction waves. Only reduction waves are discussed from now on, since the processes show a high degree of irreversibility. All potential values are given in Table II.

An additional 0.5 equiv of Li^+ clearly results in the observation of a total of six reduction waves, although the first one is relatively small. These six waves can be assigned to the six electrochemical processes shown in Scheme I. In order of increasing negative potential, the processes are assigned to 1″ < 1′ < 2″ < 1 < 2′ < 2. Further confirmation for these assignments comes from the voltammogram recorded using 2 equiv of Li^+ per cryptand equivalent. As expected from the equilibria presented in the scheme, only two main waves are observed, those corresponding to processes 1″ and 2″ (−0.44 and −0.97 V, respectively), which are the redox processes of the 1:2 complex. Only a very small wave is observed for process 1′, a likely situation since equilibrium

Table II. Electrochemical Results for **2** in the Presence of Different Cations[a]

	equiv	E_c^1	E_a^1	E_c^2	E_a^2	$E_c^{1'}$	$E_a^{1'}$	$E_c^{2'}$	$E_a^{2'}$	$E_c^{1''}$	$E_a^{1''}$	$E_c^{2''}$	$E_a^{2''}$
Li^+	0	−1.07	−0.98	−1.48	−1.32								
	0.5	−1.04	−0.97	−1.46	−1.31	−0.69	−0.52	−1.31	−1.18				
	1.0	−1.04		−1.46		−0.70	−0.49	−1.27	−1.15	−0.44		−0.97	−0.80
	2.0					−0.71				−0.44	−0.36	−0.97	−0.88
Na^+	0.5	−1.07	−1.01			−0.91	−0.84	−1.36	−1.25				
	1.0					−0.92	−0.85	−1.38	−1.24				
	2.0					−0.92	−0.85	−1.37	−1.24	−0.71		−1.16	−0.99
K^+	0.5	−1.07	−0.98	−1.45	−1.32	−0.92	−0.80	−1.45	−1.32				
	1.0					−0.96	−0.79	−1.45	−1.35				
	2.0					−0.96		−1.45	−1.36	−0.82			

[a] Subscripts c and a refer to cathodic and anodic peaks, respectively. All values are reported in volts, relative to a Ag/AgCl reference electrode. Empty entries mean that those values were impossible to measure from the voltammograms.

Table III. Cation Binding Enhancements Resulting from Electrochemical Reductions of **2**[a]

	K_3/K_1	K_5/K_3	K_4/K_2	K_6/K_4
Li^+	8.2×10^5	3.4×10^2	5.6×10^5	1.2×10^5
Na^+	7.5×10^2	1.1×10^2	3.5×10^3	
K^+	7.5×10^2		2.3×10^2	

[a] The Li^+ values were calculated using the cathodic waves while the Na^+ and K^+ values were calculated using the standard potentials. All are reported as the ratio of the corresponding equilibrium constants. K_3/K_1 and K_5/K_3 were calculated from the 1:0.5 L:M^+ experiments while the K_4/K_2 and K_6/K_4 values were obtained from the 1:1 experiments.

K_2 is not expected to be shifted totally to the right. This is the first example of electrochemical and ESR characterization of a 1:2 ligand:Li^+ complex using an anthraquinone macrobicycle.

Electrochemical results for **2** in the presence of Na^+ are summarized in Table II and presented in Figure 6. A clear and reversible redox process corresponding to 1′ was observed for the complete series from 0.5 to 2 equiv of added Na^+. Based on the observation of only two, reversible and of equal intensity waves at the 1:1 ratio, we have assigned the one at −1.36 V to 2′, rather than to a shifted one for process 2. This is equivalent to saying that, in the presence of Na^+, process 2 is totally inhibited by competition with equilibrium K_3. Therefore, processes 1′, 1, and 2′ are seen for the 1:0.5 ratio solution, but only 1′ and 2′ are seen for the 1:1 case. Addition of an extra 1 equiv of Na^+ results in yet another reduction wave, which is irreversible; see Figure 6. This wave, which appears at a potential of −0.71 V, is assigned to the 1″ process of the 1:2 complex. As discussed in ESR Experiments, this 1:2 complex is probably of the type where one of the cations is inside of the cavity while the other interacts with the outside carbonyl of the quinone. Since the latter cation is probably in very fast exchange with the medium, it was not possible to resolve a splitting in the ESR experiment, mainly due to the broadening induced by the process, but its time average effect on the electron affinity of the complex is easily detected in the voltammetric experiment. Notice that a reasonably reversible couple is observed at −1.08 V, which is assigned to process 2″.

The voltammetric results with K^+ are similar to those obtained with Na^+, except for the actual numerical values of the potentials. These can be found in Table II. One other difference is that processes 2 and 2′ have very similar potentials, so they are overlapped.

Binding enhancements resulting from electrochemical reduction of cryptand **2** have been calculated for the cases where the potentials were measured. These results are summarized in Table III.

As has been previously observed, the largest K_3/K_1 enhancement is observed for Li^+, a reflection of the strong electrostatic interaction between the anion radical and this very charge dense cation.[1-9] The corresponding enhancement for the Na^+ and K^+ cases are the same, and much smaller than the one for Li^+. This enhancement of 7.5×10^2 for K^+ (K_3/K_1) is the largest ever observed for any of the anthraquinone ligands that we have studied. Such an observation is probably the result of the good correspondence between the cavity size and the cation diameter. Nevertheless, this ligand is exhibiting the leveling effect mentioned in the Introduction; that is, upon reduction it is not exhibiting high binding selectivity for any of the cations.

Binding of the second cation is also dramatically enhanced via electrochemical switching, especially for the Li^+ case. This is evident from the very large (10^5) values for both K_4/K_2 and K_6/K_4. The order observed for K_4/K_2 is exactly the one anticipated on the basis of the charge densities, with $Li^+ > Na^+ > K^+$.

Binding Constant Determinations. These experiments were conducted for two reasons: First, confirmation of the existence of (**2**:2Li^+) was desired. This should be feasible by binding measurements, especially by a ^7Li NMR titration. Second, absolute values of the binding constants were desired, not just their relative ratios as reported in Table III.

The chemical shift (δ) vs $[\mathbf{2}]_{tot}/[M^+]_{tot}$ plots are presented in Figure 7. Part a corresponds to the Na^+ titration, while part b corresponds to the Li^+ titration. It is clear that the graph for the Na^+ case shows two almost perfectly linear segments, with the slope transition occurring at a value of 1. This behavior indicates the formation of a very strong 1:1 complex between the cryptand and Na^+. Actually, the value for K_1 is too large to be measured by the NMR technique, since the contribution to δ from the free cation resonance is negligible at all concentration ratios studied. No curvature is noted for ratios below 1, not even around the 0.5 value, which corresponds to a 1:2 stoichiometry. Although the numerical value of K_1 determined by a nonlinear regression program was not accurate, it was possible to obtain a very good fit of the data if $K_2 = 0$. When a value of K_2 different from 0 was added, the computer fit was always much worse. This means that a model which assumes only 1:1 complex formation is able to fit the data better.

The situation observed for the Li^+ titration is quite different; see Figure 7b. In this case the portion of the plot below a concentration ratio of 1 clearly exhibits curvature. A good computer fit was obtained when a $K_2 \neq 0$ was used in the fitting process. Contrary to the sodium case discussed above, the fit is poor if $K_2 = 0$. The value of K_1 from the best fit by the nonlinear regression treatment was 4.1×10^4, and that for K_2 was 1.7×10^2; see Table IV.

Since the value of K_1 for **2**:Na^+ was too large for a reasonable estimation via NMR spectroscopy, binding determinations for Na^+ and K^+ were conducted via the potentiometric titration method using Ag^+. This method was calibrated by determining the Ag^+, Na^+, and K^+ binding with cryptand [2.2.2] (Table IV) and compared with literature values.[17] The values determined were 3.8×10^5 and 1.7×10^6 for Na^+ and K^+, respectively; see Table IV. As expected, these values are much smaller than the corresponding ones for the same cations binding with [2.2.2]. The cavity in **2** is not as well suited as that of [2.2.2] to completely envelop the cation in a symmetric way. From CPK models the cavity of **2** is somewhat smaller than that of [2.2.2]. Also as anticipated, the relative binding order of **2** increased in the following order: $Li^+ < Na^+ < K^+$.

Upon reduction of **2** to $\mathbf{2}^{\bullet-}$, the highest binding enhancement is observed for Li^+, the binding constant of which increases up

(17) Cox, B. G.; Garcia-Rosas, J.; Schneider, H. *J. Am. Chem. Soc.* **1981**, *103*, 1384.

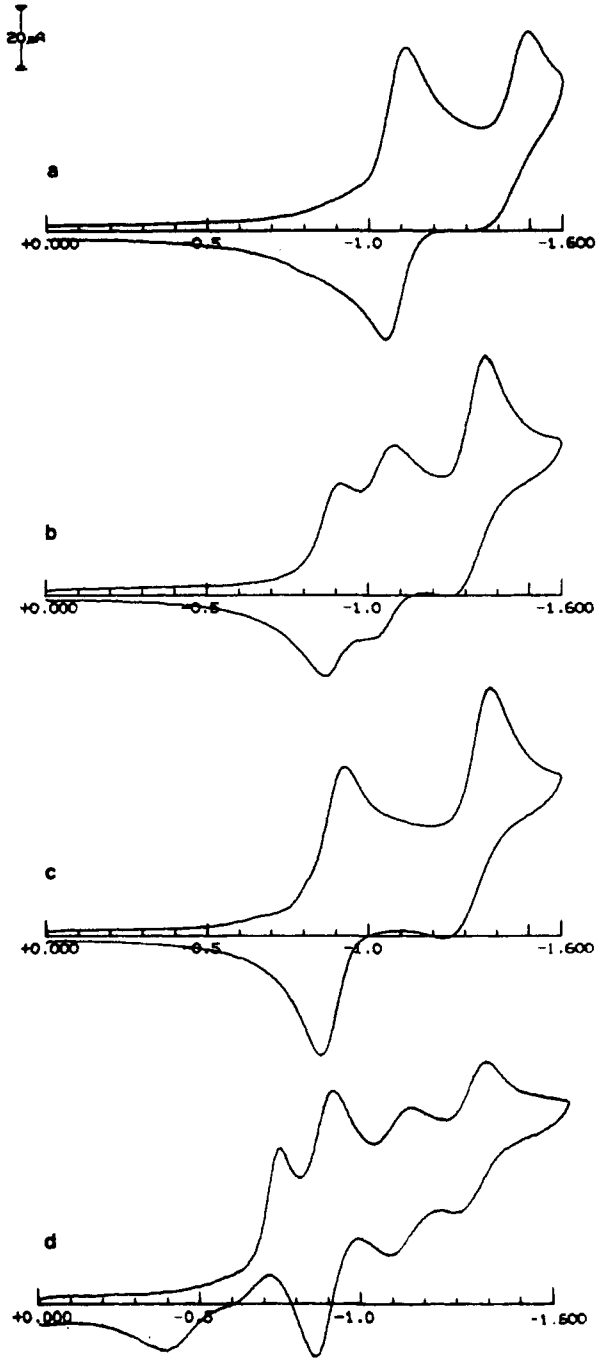

Figure 6. Cyclic voltammograms for **2** in CH_3CN–TBAP as a function of added $NaClO_4$: (a) no added Na^+, (b) 0.5 equiv of Na^+ added/equiv of **2**, (c) 1.0 equiv of Na^+ added, and (d) 2.0 equiv of Na^+ added. Potentials are referenced to a Ag/AgCl electrode.

to a K_3 value of 3.2×10^{10}. This value is much larger than the corresponding one for Li^+ with [2.2.2] and comparable to the ones with [2.2.1] and [2.1.1]. The values of K_3 for Na^+ and K^+ are high (in the order of 10^8–10^9) but still lower than the corresponding ones with the simple cryptands; see Table IV.

Further reduction of $\mathbf{2}^{\bullet-}$ to $\mathbf{2}^{2-}$ results in a very large enhancement for the binding with Li^+ to a K_5 value of 1×10^{13}. This value is clearly higher than any other with the simple cryptands. The K_5 value with Na^+ is still lower than the one [2.2.1]. No K_5 value was determined for K^+.

By far, the most noticeable changes in binding were observed for the **2**:2Li^+ complex. While this complex has a relatively modest stability constant of 1.7×10^2, reduction of the ligand to $\mathbf{2}^{\bullet-}$ resulted in a stability constant K_4 of 1.0×10^8. Further reduction to the dianion leads to a K_6 value of 1.3×10^{13}. The latter value is comparable to the one leading to the formation of the 1:1 complex from the dianionic ligand. These results are clearly in accord with the ESR observations, which showed the presence of $2^{\bullet-}$:2Li^+, even in the presence of 1 equiv of Li^+/equiv of anion radical. The presence of charge in the ligand leads to a very pronounced tendency to form 1:2 complexes with Li^+, consistent with the favorable geometric and electronic considerations discussed above.

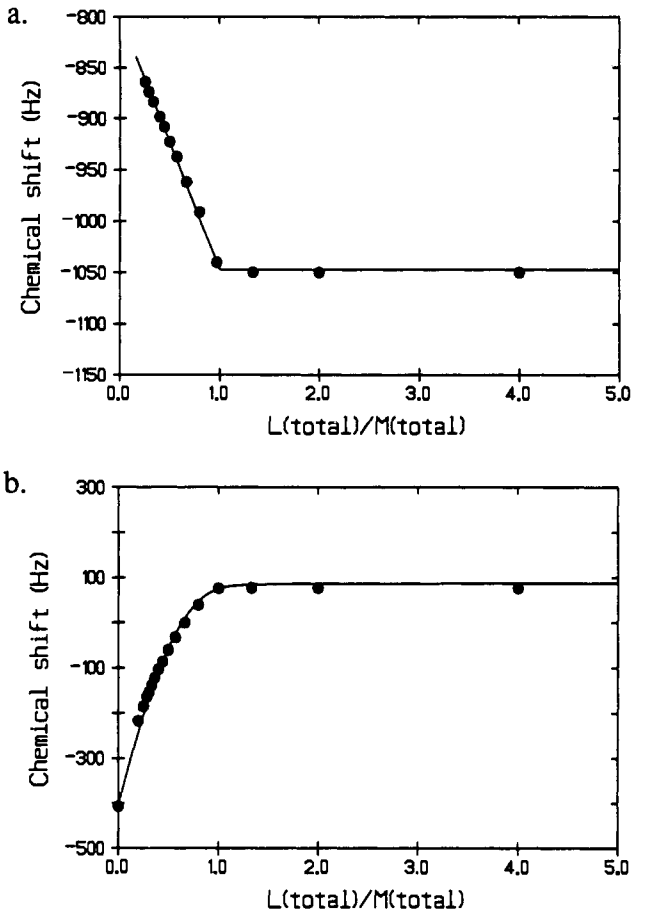

Figure 7. Plots of the alkali-metal chemical shift in hertz (δ) vs $[\mathbf{2}]_{tot}/[M^+]_{tot}$ for titrations done at constant [**2**] while adding (a) Na^+ and (b) Li^+. The solid curves represented the best fit.

Table IV. Log of the Binding Constants for Ligand **2** and Selected Cryptands with Li^+, Na^+, K^+, and Ag^+ in MeCN Determined Potentiometrically via Ag^+ Titration (Values for **2**:Li^+ and **2**:2Li^+ Determined in MeCN-d_3 Using NMR)

ligand	cation	log K_i	log K_{i+1}	method	ref
[2.1.1] (i = 1)	Li^+	>10.00 ± 0.10		pot.	*a*
[2.2.1]	Li^+	10.33 ± 0.10		pot.	*a*
(i = 1)	Na^+	11.30 ± 0.10		pot.	*a*
[2.2.2]	Li^+	6.97 ± 0.10		pot.	*a*
(i = 1)	Na^+	9.63 ± 0.10		pot.	*a*
		9.51 ± 0.07		pot.	*b*
	K^+	10.70 ± 0.10		pot.	*a*
		10.50 ± 0.08		pot.	*b*
	Ag^+	8.99 ± 0.10		pot.	*a*
		8.88 ± 0.06		pot.	*b*
2 (i = 1)	Li^+	4.61 ± 0.28	2.22 ± 0.11	NMR	*b*
	Na^+	5.58 ± 0.14		pot.	*b*
	K^+	6.22 ± 0.11		pot.	*b*
	Ag^+	5.03 ± 0.10		pot.	*b*
$\mathbf{2}^{\bullet-}$ (i = 3)	Li^+	10.5	8.0	NMR & CV	*b*
	Na^+	8.5		pot. & CV	*b*
	K^+	9.1		pot. & CV	*b*
$\mathbf{2}^{2-}$ (i = 5)	Li^+	13.0	13.1	NMR & CV	*b*
	Na^+	10.5		pot. & CV	*b*

[a] Values taken from: Cox, B. G.; Garcia-Rosas, J.; Scheneider, H. *J. Am. Chem. Soc.* **1981**, *103*, 1384. [b] This work.

Summary

A novel, redox-active cryptand containing an anthraquinone group has been studied by cyclic voltammetric and ESR techniques in the presence and absence of Li^+, Na^+, and K^+ cations. An unexpected 1:2 ($L^{\bullet-}$:2Li^+) symmetric complex was easily detected by ESR spectroscopy, even when the relative stoichiometric ratio present was only 1:1. The presence of such a complex was confirmed using cyclic voltammetry and alkali-metal NMR (both ^{23}Na and ^{7}Li). The voltammetric results show, for the first time, the direct resolution of six reduction waves, two for each of the ligand states. These are the free ligand, the 1:1 complex, and the 1:2 complex. Previously, a maximum of only four resolved reductions had been observed for an anthraquinone podand.[5] The structure of this 1:2 complex probably involves an interaction of the two Li^+ cations with the anthraquinone carbonyl that points to the inside of the cryptand cavity. Based on CPK models, it is possible for the two cations to each "sit" comfortably on two "pockets" created by the crown around this carbonyl. This proposal is structurally in accord with previous ESR observations involving **4**, which showed that two Na^+ can interact with the same carbonyl while being enveloped by two podand side arms.

ESR and voltammetry also provide evidence for 1:2 complexes between $\mathbf{2}^{\bullet-}$ and Na^+ or K^+. ESR spectral changes associated with 1:2 complex formation include increased line broadening and redistribution of spin density, as reflected by hydrogen coupling constant differences. On the other hand, it was not possible to resolve more than one metal cation nuclear splitting as in the case with Li^+. These observations have been interpreted in terms of a 1:2 complex where one of the M^+ is cryptated and the other one is interacting with the external carbonyl on the anthraquinone. The latter is probably in fast exchange with the solvent; thus, it is not possible to resolve its splitting, but it can lead to appreciable line broadening. Such 1:2 complexes were detected by cyclic voltammetry as well. For the 1:1 complex of the anion radical with K^+, it was not possible to return the ESR spectrum back to that of the free anion radical upon addition of cryptand [2.2.2]. This indicates that the complex formed by $\mathbf{2}^{\bullet-}$:K^+ is at least as strong as that formed by [2.2.2]:K^+.

Acknowledgment. We thank the National Institutes of Health for Grant GM 33940 which supported this work. We wish to also thank the National Science Foundation, Division of Chemistry Grant No. CHE-9011901, for partial support. We also thank Dr. Rosario Concepcion for simulating the ESR spectrum for the species with sodium.

Registry No. 2, 137571-97-2; $\mathbf{2}^{\bullet-}$, 137571-98-3; $\mathbf{2}^{\bullet-}$·2Li^+, 137572-00-0; $\mathbf{2}^{\bullet-}$·2Na^+, 137572-01-1; $\mathbf{2}^{\bullet-}$·2K^+, 137572-02-2; $\mathbf{2}^{\bullet-}$·Li^+, 137572-03-3; $\mathbf{2}^{\bullet-}$·Na^+, 137572-04-4; $\mathbf{2}^{\bullet-}$·K^+, 137572-05-5; $\mathbf{2}^{2-}$, 137571-99-4; 4,13-diaza-18-crown-6, 23978-55-4; 1,8-bis(2-bromoethoxy)anthraquinone, 69595-68-2; 1,8-dihydroxyanthraquinone, 117-10-2; cryptand[2.2.2]·Na^+, 32611-94-2; cryptand[2.2.2]·K^+, 61624-59-7; cryptand[2.2.2]·Ag^+, 57692-62-3.

In Situ Atomic Force Microscopy of Underpotential Deposition of Ag on Au(111)

Chun-hsien Chen, Scott M. Vesecky, and Andrew A. Gewirth*

Contribution from the Department of Chemistry, University of Illinois, 505 South Mathews Avenue, Urbana, Illinois 61801. *Received August 8, 1991*

Abstract: Atom-resolved atomic force microscope (AFM) images of underpotentially deposited (upd) monolayers of Ag on Au(111) are presented. These images show that the structure of this monolayer is dependent on the nature of the electrolyte in which the upd process occurs. Specifically, Ag shows a 3 × 3 overlayer in sulfuric acid and a 4 × 4 overlayer in nitrate- and carbonate-containing electrolytes. In perchloric acid a more complex structure is observed which, like the sulfate and nitrate systems, is also not close packed. In acetate, a close-packed monolayer is formed. The different monolayer structures give rise to packing densities which correlate with electrolyte size, except in the case of perchloric acid. However, there is little agreement between packing densities predicted from coulometric measurements and those actually observed with the AFM. The discrepancy between the two measurements is ascribed to differing amounts of charge transfer between electrolyte and adatom which alters the amount of charge needed for upd lattice formation.

1. Introduction

The focus of electrochemical surface science is correlation of electrode surface structure with electrochemical reactivity. Much attention in this area has centered on the underpotential deposition (upd) process,[1-3] in which a monolayer or submonolayer of a foreign metal adatom is deposited at potentials positive from the reversible Nernst potential. Upd can be thought of as the formation of a substrate-adatom bond before the formation of a somewhat weaker adatom-adatom bond during bulk deposition. The monolayers formed during the upd process are interesting not only because of their physical properties which are different from bulk phases of either the surface or the adatom, but also because they exhibit catalytic activity toward the electrooxidation of small organic molecules.

A central focus of studies of the upd process is the structure of the metal adsorbate on the surface. While this aspect has been addressed extensively via both in situ and ex situ methods, direct confirmation of the monolayer structure has been elusive. Scanning tunneling microscope (STM) measurements[4] have provided substantial new information about upd,[5] but atomic resolution has been achieved in only a few upd systems.[6-8]

* To whom correspondence should be addressed.

(1) Kolb, D. M. In *Advances in Electrochemistry and Electrochemical Engineering*; Gerischer, H., Tobias, C. W., Eds.; Wiley-Interscience: New York, 1978; Vol. 11, pp 125-271.

(2) Adzic, R. In *Advances in Electrochemistry and Electrochemical Engineering*; Gerischer, H., Tobias, C. W., Eds.; Wiley-Interscience: New York, 1984; Vol. 13, pp 159-260.

(3) Juttner, K.; Lorenz, W. J. *Z. Phys. Chem. (Wiesbaden)* **1980**, *122*, 163.

(4) Reviews: (a) Sonnenfeld, R.; Schneir, J.; Hansma, P. K. In *Modern Aspects of Electrochemistry*; White, R. E., Bockris, J. O'M., Conway, B. E., Eds.; Plenum: New York, 1990; Vol. 21, pp 1-28. (b) Cataldi, T. R. I.; Blackham, I. G.; Briggs, G. A. D.; Pethica, J. B.; Hill, H. A. O. *J. Electroanal. Chem. Interfacial Electrochem.* **1990**, *290*, 1-20.

(5) (a) Green, M. P.; Hanson, K. J.; Carr, R.; Lindau, I. *J. Electrochem. Soc.* **1990**, *137*, 3493-3498. (b) Green, M. P.; Hanson, K. J.; Scherson, D. A.; Xing, X.; Richter, M.; Ross, P. N.; Carr, R.; Lindau, I. *J. Phys. Chem.* **1989**, *93*, 2181-2184.

0002-7863/92/1514-451$03.00/0